

Synthesis and characterization of mixed ligand complexes of Fluconazole drug and glycine with some transition metals: antifungal study

Yasmin M.S. Jamil ¹*, Majeda M. Al-Baseer¹, Basem Al-Akhali² and Ahmed N. Alhakimi^{3,4}

¹Department of Chemistry, Faculty of Science, Sana'a University, Sana'a, Yemen,

²Department of Microbiology, Faculty of Science, Sana'a University, Sana'a, Yemen,

³Department of Chemistry, Faculty of Science, Ibb University, Ibb, Yemen,

⁴Department of Chemistry, Faculty of Science, Qassim University, Qassim, Buraidah, Saudi Arabia

*Corresponding author: y.jamil@su.edu.ye

ABSTRACT

Mixed ligand complexes of fluconazole (FCZ), like the main ligand and glycine (Gly) as the secondary ligand, were synthesized and characterized using elemental analysis, spectroscopy, infrared and electronic spectra, magnetic susceptibility, and molar conductivity. The results showed that 1:1:1 [M:L1:L2] octahedral complexes were formed, with FCZ coordinating through its C=N group and glycine coordinating through its carboxylic oxygen and amino nitrogen. Molar conductivity indicated the complexes were not electrolytic in nature. The antifungal activity of FCZ, glycine, and their metal complexes with Cu, Ni, and Cd was tested against *Aspergillus niger*, *Penicillium italicum*, and *Candida albicans*. Cadmium complex [Cd(FCZ)(Gly)(H₂O)₂Cl].2H₂O showed significantly enhanced activity with outperforming the standard antifungal agent Nystatin against *A. niger* and *P. italicum*. These findings highlight the potential of such complexes as effective antifungal agents.

ARTICLE INFO

Keywords:

Propagation, Intensity, Phase, Beam, Distribution of Beam

Article History:

Received: 19-January-2025,

Revised: 9-February-2025,

Accepted: 8-March-2025,

Available online: 30 April 2025.

1. INTRODUCTION

Numerous studies have focused on the reactions mediated by metal ions involving nucleic acid constituents and amino acid side chains [1, 2]. Such reactions are valuable for understanding metalloenzyme interactions in vivo [3]. The azole class of compounds serves as an important category of antimicrobial agents [4], and current research primarily aims at developing azole medications [5]. Several azole-based antimicrobial agents, including ketoconazole, econazole, miconazole, posaconazole, fluconazole, voriconazole, and savuconazole, are used clinically [4, 5, 6]. There is a wealth of scientific literature documenting the interactions between various triazole compounds and metallic cations [7, 8, 9, 10]. These studies mainly focus on identifying and characterizing these interactions, defining the structural configurations formed by the resulting coordination complexes, and examining

the functional groups that interact directly with the metal ions. Some research has also explored the effects of metal ions on antibacterial activity [11, 12]. Fluconazole (FLZ) [13], chemically identified as 2-(2,4-difluorophenyl)-1,3-bis(1H-1,2,4-triazol-1-yl)-2-propanol (Fig. 1), is a synthetic triazole-based antifungal agent. It demonstrates broad-spectrum activity and has been clinically proven effective against various systemic and superficial fungal infections, making it a first-line antifungal treatment. Fluconazole is widely used for both treating and preventing disseminated candidiasis and deep-seated organ infections caused by pathogenic fungi. Its effectiveness, along with a favorable pharmacokinetic profile, has established it as a cornerstone in managing invasive and opportunistic fungal diseases [14]. Fluconazole exerts its antifungal activity by selectively inhibiting the fungal enzyme 14 α -demethylase, which is critical in the ergosterol

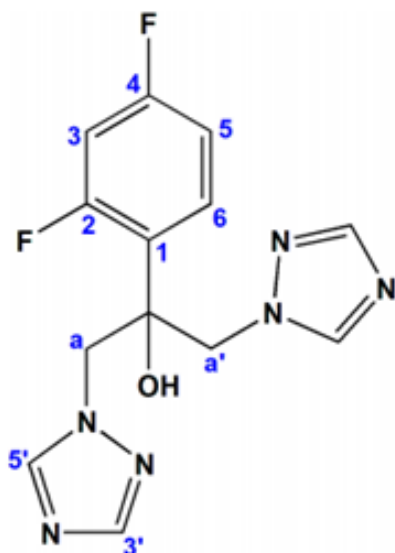


Figure 1. Chemical structure of fluconazole

biosynthesis pathway. This enzyme catalyzes the conversion of lanosterol to ergosterol, a vital component of the fungal cell membrane. By inhibiting 14 α -demethylase, fluconazole disrupts this biosynthetic pathway, leading to an accumulation of 14 α -methyl sterols and a subsequent depletion of ergosterol. This change in membrane composition compromises both membrane integrity and function, ultimately inhibiting fungal growth and replication. Importantly, fluconazole has a significantly higher affinity for fungal 14 α -demethylase compared to its mammalian counterparts, which explains its selective toxicity toward fungal cells while sparing those of mammals. This differential sensitivity is essential for the therapeutic effectiveness of fluconazole in treating fungal infections [15].

To enhance our understanding of the underlying mechanisms, we found it essential to investigate the interactions between fluconazole, the amino acid glycine, and biologically relevant metal ions such as Cu(II), Ni(II), and Cd(II). These studies are crucial for exploring potential coordination chemistry, binding affinities, and their biological implications, which may provide valuable insights into the pharmacological and biochemical behavior of these compounds in the presence of metal ions. We synthesized complexes as model systems to simulate the potential interactions and coordination behavior of fluconazole (FCZ) with metal ions in biological environments. The synthesized complexes were thoroughly characterized using various analytical techniques, including elemental analysis, conductivity measurements, infrared (IR) spectroscopy, electronic (UV-Vis) spectroscopy, and magnetic susceptibility studies. Based on the spectroscopic and analytical data, we determined the bonding modes of the ligands. Fluconazole was found to act as a neutral monodentate ligand, coordinating with the metal ions through its C=N group under the experimental conditions.

In contrast, the amino acid glycine served as a bidentate ligand, coordinating via the carboxylate oxygen and the amino nitrogen atoms. Collectively, the data support the suggestion of an octahedral geometry for the metal chelates, which is consistent with the observed coordination behavior and spectral properties.

2. MATERIALS AND METHODS

2.1. MATERIALS

Reference The fluconazole (FCZ) sample employed in this investigation was kindly supplied by Saba Pharma. Pharmaceuticals and Chemicals Company Limited. All chemicals and reagents employed in this study were of analytical grade and obtained from reputable suppliers (BDH and Scharlau), ensuring high purity and consistency throughout the experimental procedures. $\text{CuCl}_2 \cdot 2\text{H}_2\text{O}$, $\text{NiCl}_2 \cdot 6\text{H}_2\text{O}$, $\text{CdCl}_2 \cdot \text{H}_2\text{O}$, glycine, NaOH, DMSO, CH_2OH , $\text{C}_4\text{H}_{10}\text{O}$, and distilled water.

2.2. PREPARATION OF THE METAL COMPLEXES

A hydroalcoholic solution containing 0.1 M fluconazole (FCZ) and 0.1 M glycine was prepared, along with 0.1 M solutions of each metal chloride salt (Fig. 2). In a round-bottom flask, 5.0 mL of an alcoholic FCZ solution was combined with 5.0 mL of an aqueous glycine solution. The mixture was stirred thoroughly, after which 5.0 mL of the respective metal salt solution was added dropwise under continuous stirring. The reaction mixture was then refluxed for 3 to 4 hours at 80 °C on a hot plate using a magnetic stirrer. During the reflux process, solid complexes formed visibly at the bottom of the flask. After cooling, the mixture was filtered via Whatman filter paper, and the resulting precipitate was sequentially washed with hot methanol, hot distilled water, and diethyl ether, respectively., followed by air-drying for one to three days. The used synthetic procedure steps were the same except for changing the metal salt and adjusting the pH according to the type of prepared complex. Prepared complexes were colored except that of cadmium. The colors of the synthesized metal complexes are summarized in Table 1.

2.3. SPECTRAL MEASUREMENTS

At the Yemen Standardization and Metrology Organization, the complexes were analyzed using infrared (IR) spectroscopy, with measurements conducted in the wavenumber range of 400–4000 cm^{-1} by employing FTIR-4800S (Shimadzu, Japan) equipment. The electronic spectra of the synthesized complexes were recorded within the wavelength range of 400–800 nm employing a UV-Vis spectrophotometer. (specord40, Analytik Jena, Germany) at the Yemen Standardization and

Table 1. Some physical properties and Elemental Analysis of Metal complexes

Complex	Color (Yield)	M.P. (C°)	$\Delta m (\Omega^{-1} \text{ cm}^2 \text{ mol}^{-1})$	F. Wt(g/mole)	Element Analysis Calculated% (Found)			
					%C	%H	%N	%M
[Cu(FCZ)(Gly)(H ₂ O) ₂ Cl].2H ₂ O	Sky blue 69.67	236	23.8	551.21	32.65 (32.72)	4.35 (4.14)	17.78 (17.81)	11.52 (11.20)
[Ni(FCZ)(Gly)(H ₂ O) ₂ Cl].2H ₂ O	Bluish green 30.74	>300	27.7	546.35	32.95 (32.95)	4.39 (4.44)	17.94 (18.03)	10.74 (10.62)
[Cd(FCZ)(Gly)(H ₂ O) ₂ Cl].2H ₂ O	White 70.61	240	12.2	600.07	29.99 (29.91)	3.99 (3.85)	16.34 (16.33)	18.73 (18.81)

Metrology Organization. The metal content was measured by using VARIAN ICP-OES at Yemen Standardization and Metrology Organization. Standard solutions of metal nitrate were used for calibration. The compound's C, H, and N analyses were conducted in Vario EL Fab. CHN Nr. 11042023, at the Micro Analytical Center, Faculty of Science, Cairo University, Egypt. The weight loss methods were used to determine the coordinated and uncoordinated water contents gravimetrically.

2.4. PHYSICAL MEASUREMENTS

The molar conductivity of 10^{-1} M solutions of the Cu(II), Ni(II), and Cd(II) complexes was determined in dimethyl sulfoxide (DMSO) as the solvent by means of a Jenway conductivity meter (Model 4510). Measurements were carried out at room temperature on freshly prepared solutions to ensure accuracy. Additionally, the melting points of the ligand and its corresponding complexes were measured using a Stuart Scientific electrothermal melting point apparatus. Melting points in glass capillary tubes in degrees Celsius.

2.5. BIOLOGICAL SCREENING

Three fungi strains (*Aspergillus niger* 16404, *Penicillium italicum* 10129, and *Candida albicans* 10231) were used to test the antifungal properties of the FCZ and glycine complexes. The agar well diffusion method was employed to assess the antimicrobial activity [16]. The antifungal activity was evaluated using dimethyl sulfoxide (DMSO) as the solvent to prepare stock solutions at a concentration of 500 $\mu\text{g/ml}$. This solution was then utilized to prepare different concentrations, which included 2.5, 5, 10, 50, and 100 $\mu\text{g/ml}$, respectively. The nutrient agar's surface was infected with the microorganisms. The wells and ditches made on the agar plates were inoculated with the different concentrations of the compounds and repeated three times for each concentration. Nystatin at a concentration of 100 $\mu\text{g/mL}$ was employed as a reference standard. All Petri dishes were incubated at 37°C for 24 hours to allow for optimal microbial growth and activity assessment. By determining the inhibitory zone's diameter (mm), the average results for each con-

centration were recorded.

3. RESULTS AND DISCUSSION

The synthesized Cu(II), Ni(II), and Cd(II) complexes with the ligands fluconazole (FCZ) and glycine (Gly) were obtained in pure form following sequential washing with methanol, distilled water, and diethyl ether. All the complexes were colored except the Cd(II) complex, which exhibited stability under atmospheric conditions, was insoluble in water, and demonstrated limited solubility in most organic solvents, but all were soluble in DMSO. Ni (II) complex had the highest melting point (> 300°C), and the Cu (II) Cd (II) complexes had melting points of 236°C and 240°C, respectively. The molar conductivity of the synthesized complexes was measured in dimethyl sulfoxide (DMSO) at room temperature. The results indicated that the Cu (II), Ni (II), and Cd (II) complexes with (FCZ, Gly) had a molar conductance of 23.8, 27.7, and 12.2 ($\text{S} \cdot \text{mol}^{-1} \cdot \text{cm}^2$), respectively. The data indicate that these chelates exhibit anionic characteristics. Our results are consistent with what is reported in the literature [7, 8].

3.1. IR SPECTRA STUDIES

The infrared (IR) spectra of fluconazole (FCZ), glycine, and their corresponding metal complexes (Figs 3-8) exhibit distinctive band positions, shifts, and intensities, reflecting monodentate coordination of FCZ and bidentate chelation of glycine. The key findings are that a band attributed to C=N stretching at 1614 cm^{-1} in free FCZ shifts to 1624, 1621, and 1641 cm^{-1} in complexes, confirming Coordination occurs via the nitrogen atom [7, 9, 17]. Broad OH bands in all complexes suggest limited involvement of hydroxyl groups in coordination, while water of crystallization contributes to the broad OH absorption near (3400 cm^{-1}). The NH_2 group ($3153\text{--}3104 \text{ cm}^{-1}$) in free glycine is deprotonated to NH ($3333\text{--}3122 \text{ cm}^{-1}$) upon complexation, indicating nitrogen's involvement in coordination. The carboxyl group ($-\text{COO}^-$) displays shifts in asymmetric and symmetric stretches with a band difference of $63\text{--}76 \text{ cm}^{-1}$, confirming non-selective metal ion chelation [18, 19]. Low-intensity bands were observed in the far-infrared region ($438\text{--}670 \text{ cm}^{-1}$). These bands

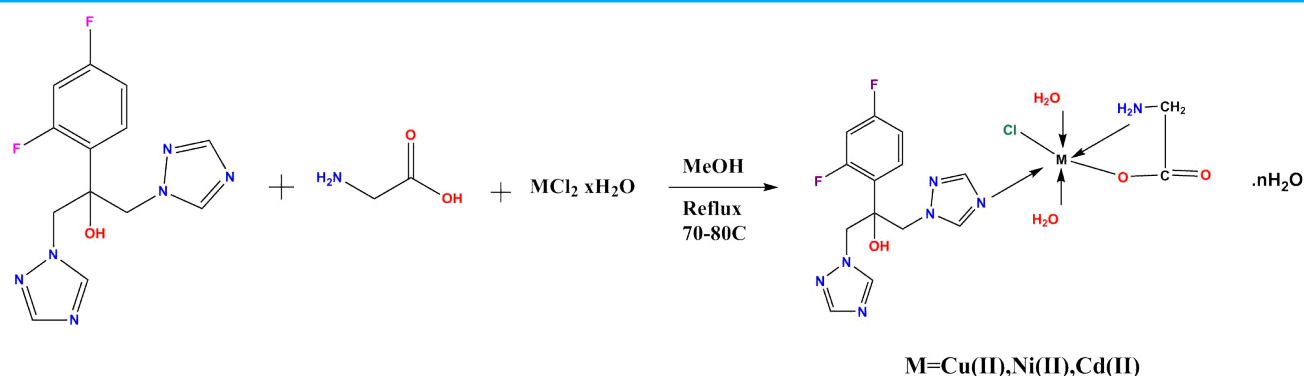


Figure 2. Synthesis of metal complexes of fluconazole and Glycine

Table 2. IR absorption bands of the FCZ, Glycine and their complexes

Compound	OH&CH	NH ₂ (N-H)	C=N, C=C	-COO, asym	-COO, sym.	C-N & C-C	M-O&M-N
FCZ	3450 3028	—	1614	—	—	1275	—
Glycine	3467	3153 3104	—	1583	1493	1323	—
[Cu(FCZ)(Gly)(H ₂ O) ₂ Cl] · 2H ₂ O	3467	3333 3160	1624	1520	1424	1213	670 524
[Ni(FCZ)(Gly)(H ₂ O) ₂ Cl] · 2H ₂ O	3467	3122	1621	1503	1431	1278	663 594 438
[Cd(FCZ)(Gly)(H ₂ O) ₂ Cl] · 2H ₂ O	3457	3201 3125	1628	1507	1420	1285	663 580 514

are assigned to the stretching vibrations of metal-oxygen $\nu(\text{M-O})$ and metal-nitrogen $\nu(\text{M-N})$ bonds. Supporting coordination through oxygen and nitrogen atoms [7, 17].

3.2. THE UV-VIS SPECTRA

The UV-Vis spectrum of the FCZ ligand exhibited a strong, sharp, and high-intensity absorption band at 275 nm (36363 cm^{-1}), which is likely attributed to a $\pi \rightarrow \pi^*$ electronic transition [7], (Figure 9 and Table 3). The UV-Vis absorption spectrum of the glycine (Figure 10) displayed a sharp, high-intensity absorption band at 278 nm (36363 cm^{-1}), which is attributed to an $n \rightarrow \pi^*$ electronic transition involving functional groups such as -O-H, -C-O, -C-N, and -C=O. [20, 21] The electronic absorption spectrum of the copper(II) complex, corresponding to the Cu(II) d^9 configuration (Term 2D), exhibited three distinct bands (Fig. 11). The first two high-intensity bands were observed at 257 nm (38910 cm^{-1}) and 242 nm (41322 cm^{-1}), which are assigned to $\pi \rightarrow \pi^*$ and $n \rightarrow \pi^*$ electronic transitions, respectively. Upon comparing these bands with those of the free ligands, a noticeable shift to lower wavelengths was observed. Additionally, a new broadband appeared at 639 nm (15649 cm^{-1}), character-

istic of a d-d electronic transition of the type [$^2E_g \rightarrow ^2T_{2g}$]. These spectral changes provide strong evidence for the coordination of the ligands to the copper (II) ion. The measured magnetic moment of the complex is 1.76 Bohr magnetons (B.M.), which aligns well with the theoretically calculated value of 1.73 B.M. This agreement supports the proposed octahedral geometry around the copper (II) ion. [8, 22, 23, 24]. The Ni(II) complex, corresponding to the d^8 configuration (Term 3F), exhibits paramagnetic behavior at room temperature with an effective magnetic moment (μ_{eff}) of 2.28 Bohr Magnetons (B.M.), as shown in Table 3. This value is consistent with an octahedral geometry and indicates the presence of two unpaired electrons, as expected for a six-coordinated, high-spin Ni(II) species. In the electronic spectrum of the Ni(II) complex (Figure 12), two peaks appear at 284 nm (35211 cm^{-1}) and 273 nm (36630 cm^{-1}), which may be attributed to the ligands field transitions, which shifted to increase and lower from the two free ligands. This change gives a good indication of the complexation by ligands to the nickel (II). The absorption band at 374 nm (26738 cm^{-1}) is assigned to charge transfer $L \rightarrow M$. Additionally, two distinct absorption peaks are observed at 594 nm (16835

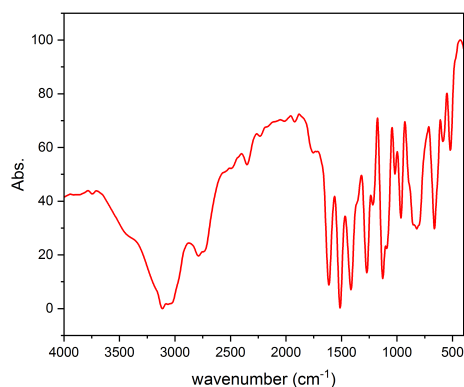


Figure 3. Infrared Spectrum of FCZ ligand

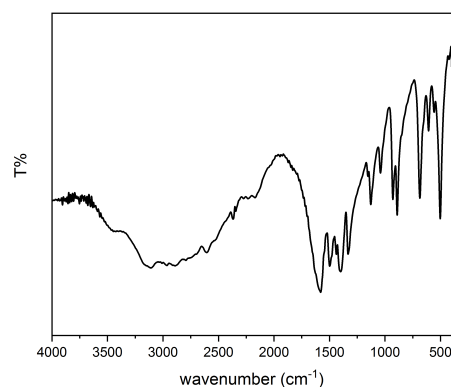


Figure 4. Infrared Spectrum of Glycine ligand

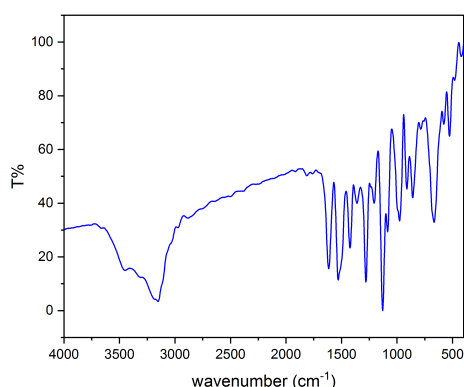


Figure 5. Infrared Spectrum of Cu (II)-FCZ,Gly Complex

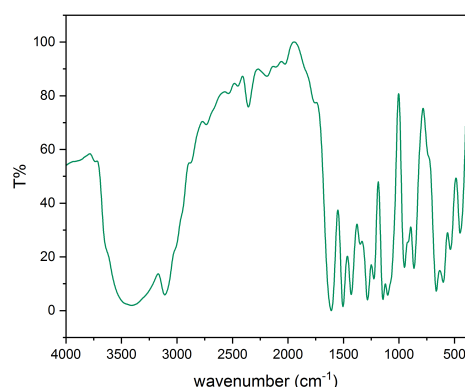


Figure 6. Infrared Spectrum of Ni (II)-FCZ,Gly Complex

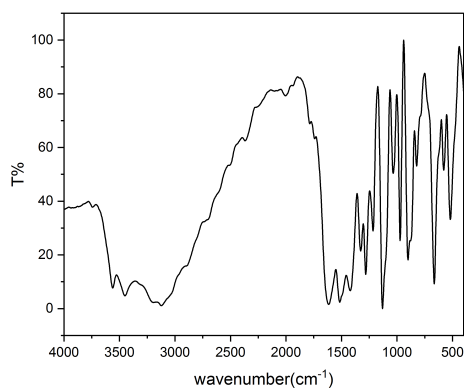


Figure 7. Infrared Spectrum of Cd (II)-FCZ, Gly complex

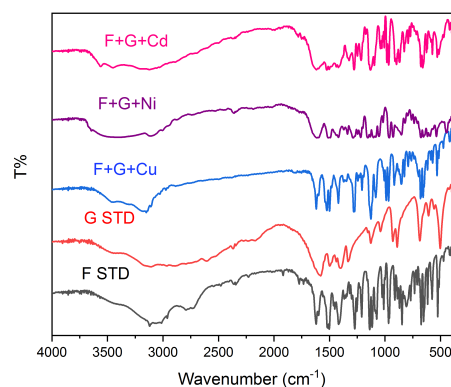


Figure 8. Infrared Spectrum of FCZ, Glycine ligands and their metal Complexes

cm^{-1}) and 996 nm (10840 cm^{-1}), corresponding to ν_3 and ν_2 transitions, respectively, as detailed in Table 3. These transitions may be appointed as ${}^3\text{A}_{2g}(\text{F}) \rightarrow {}^3\text{T}_{2g}(\text{P})$ and ${}^3\text{A}_{2g}(\text{F}) \rightarrow {}^3\text{T}_{1g}(\text{F})$ [7, 19, 24]. The Cd(II) complex, as outlined in Table 3 and Figure 13, exhibited diamagnetic behavior, consistent with its d^{10} electronic configuration, and no absorption peaks were observed in the visible region. However, absorption bands were detected at 361 nm (27700 cm^{-1}), which are attributed to charge trans-

fer $\text{L} \rightarrow \text{M}$ transitions, as illustrated in Figure 14, which is consistent with the proposed octahedral geometry of the complex [8, 25, 26].

3.3. X-RAY DIFFRACTION

At room temperature, the sample was analyzed using Cu $K\alpha$ radiation in XRD. The complexes' XRD patterns show that they are crystalline. The diffraction patterns

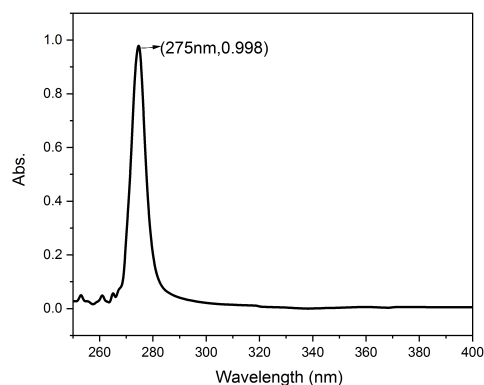


Figure 9. UV-visible Spectrum of FCZ ligand

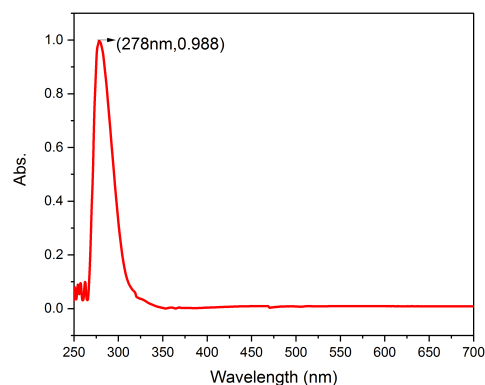


Figure 10. UV-visible Spectrum of Glycine ligand

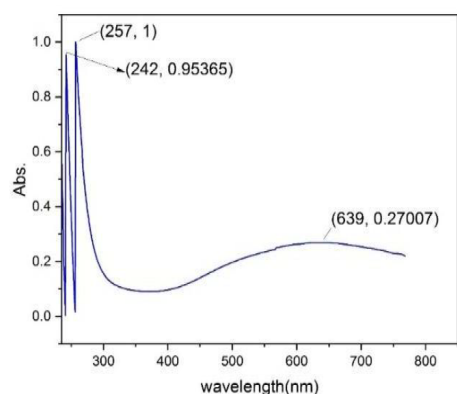


Figure 11. UV-visible Spectrum of Cu(II) complex

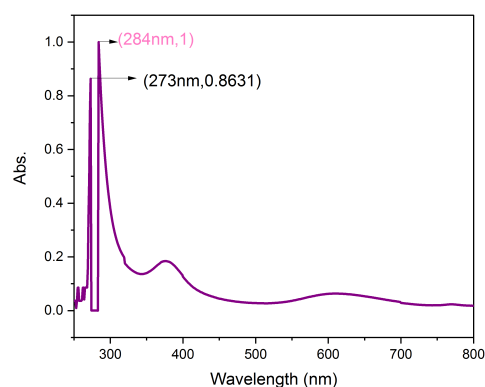


Figure 12. UV-visible Spectrum of Ni(II) complex

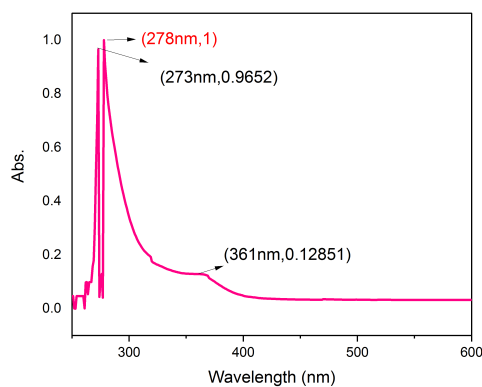


Figure 13. UV-visible Spectrum of Cd (II) complex

Table 3. Spectral properties of the prepared compounds

compound	μ_{eff} (B.M.) Cal	μ_{eff} (B.M.) found	λ_{max} (nm)	Absorption band(cm^{-1})	Assignments	Suggested Structure
[Cu(FCZ)(Gly)(H ₂ O) ₂ Cl].2H ₂ O	1.73	1.76	639	15649	$^2\text{E}_g \rightarrow ^2\text{T}_{2g}$	Octahedral
[Ni(FCZ)(Gly)(H ₂ O) ₂ Cl].2H ₂ O	2.83	2.28	374 594 987	26738 16835 10840	Charge transfer L→M $^3\text{A}_{2g}(\text{F}) \rightarrow ^3\text{T}_{1g}(\text{P})$ $^3\text{A}_{2g}(\text{F}) \rightarrow ^3\text{T}_{1g}(\text{F})$	Octahedral
[Cd(FCZ)(Gly)(H ₂ O) ₂ Cl].2H ₂ O	Diamagnetic	Diamagnetic	361	27700	Charge transfer L→M	Octahedral

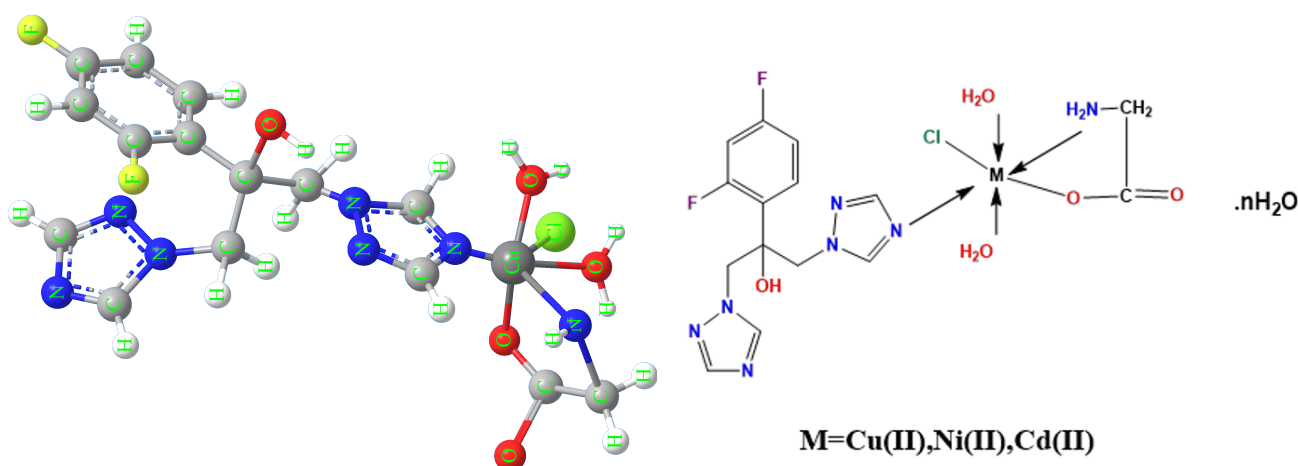


Figure 14. The proposed octahedral geometry of the prepared complexes

of both the ligands and their corresponding metal complexes were carefully obtained between 2θ , ranging from 5° to 60° . The crystallite size of the samples was determined using Scherrer's formula, expressed as $D = k \lambda / b2\theta \cos \theta$, where D represents the crystallite size, k is the Scherrer constant (taken as 0.94), λ is the wavelength of the X-ray radiation ($=0.15406$ nm), $b2\theta$ is the full width at half maximum (FWHM) of the diffraction peaks in radians, and θ is the Bragg angle. The FWHM values were obtained from the XRD patterns to calculate the average crystallite dimensions., where θ is the Bragg angle. The diffraction patterns have been successfully indexed [27]. The X-ray diffraction patterns of pure fluconazole (FCZ) are presented in Figure 15. The pure FCZ sample exhibits distinct diffraction peaks within the 2θ range of 5 – 60° , confirming its polycrystalline structure. These prominent peaks highlight the well-defined crystallinity of the FCZ sample. According to previous reports, FCZ exists in at least two polymorphic forms with slab morphologies that are granular and flake-like. The X-ray diffraction analysis revealed that the raw fluconazole (FCZ) exists as a mixture of polymorphs, as indicated by the presence of multiple distinct diffraction peaks characteristic of different crystalline phases [28]. The X-ray diffraction (XRD) analysis of pure glycine crystals was conducted using a diffractometer with Cu $K\alpha$ radiation ($\lambda = 1.5406$ Å), scanning over a 2θ range of 5° to 60° at a rate of 10° per minute. The resulting diffraction pattern, presented in Figure 15, displays sharp and well-resolved peaks at specific 2θ positions, indicative of a highly crystalline structure. These pronounced peaks demonstrate the ordered atomic arrangement and confirm the crystalline purity of the glycine sample [28]. The X-ray diffractograms of the Cu(II)-(FCZ, Glycine) metal complex are illustrated in Figure 18. A comparative analysis of the diffraction patterns for the pure FCZ (Figure 15), pure glycine (Figure 16), and the metal complex (Figure 17) reveals significant differences in their respective profiles. These variations indicate that the metal complex is

a distinct compound with a well-defined structure, rather than a simple physical mixture of the starting material. Furthermore, the Cu(II)-(FCZ, Glycine) complex exhibits diffraction peaks at various 2θ angles with reduced intensity compared to those of the pure FCZ and glycine, suggesting its crystalline nature with smaller particle dimensions. This observation supports the formation of a new chemical entity with unique structural properties [21].

3.3.1. XRD analysis of pure fluconazole

In (Figure 15), the XRD measurement result of pure FCZ can be seen. We had 5 distinct peaks, which were at 9.98° , 16.38° , 20.04° , 25.64° , and 29.20° . This was proven by the XRD, using which we had the grain sizes of the complex. (Table 4) provided the grain sizes of the ligand. The highest grain size was 53.391 nm, found at a 9.98° diffraction angle, while the lowest grain size was 31.397 nm, found at a 16.38° diffraction angle [29].

3.3.2. XRD analysis of pure glycine

Figure 16 is the XRD measurement of pure glycine. It had 5 distinct peaks, which were at 18.98° , 21.82° , 25.34° , 29.88° , and 35.90° . The XRD analysis clearly confirms that glycine exhibits a highly crystalline structure, as evidenced by its sharp and well-defined diffraction peaks. Table 4 showed the grain size of this ligand. The mean grain size was 90.32 nm [19].

3.3.3. XRD analysis of Cu (II)-FCZ-Gly Complex

Figure 17 is the XRD measurement result of the Cu (II)-FCZ-Gly complex which showed 5 distinct peaks at 9.02° , 10.54° , 14.94° , 17.48° , and 21.36° [27]. The mean grain size was 73.53 nm.

3.4. ANTIFUNGAL STUDY

Fluconazole (FCZ) is widely recognized as an effective antifungal agent, which has led to increased inter-

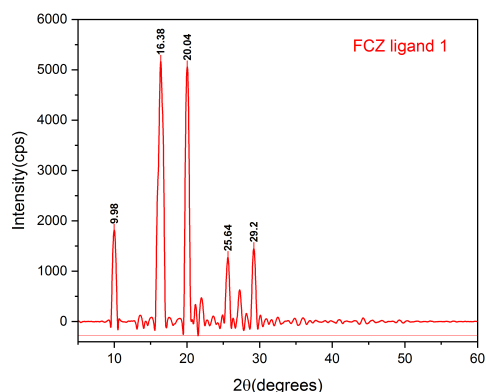


Figure 15. XRD patterns of pure FCZ.

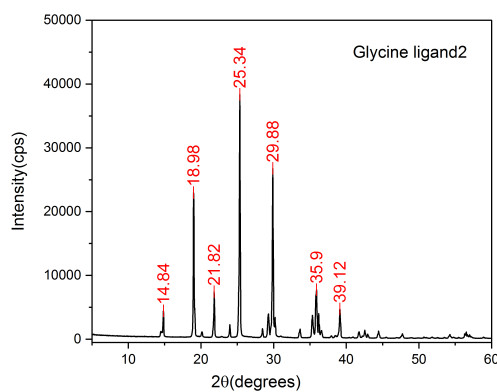


Figure 16. XRD patterns of pure Glycine.

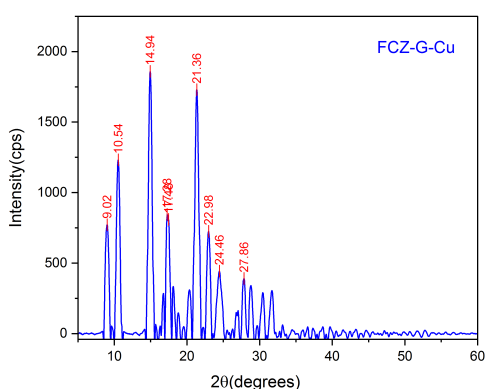


Figure 17. XRD patterns of Cu (II) complex.

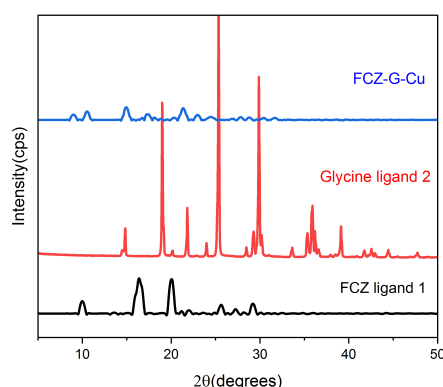


Figure 18. X-ray diffraction patterns of FCZ, Glycine ligands and Cu (II) complex.

est in developing transition metal complexes that incorporate nitrogen-donor ligands. The goal is to create metal-based drugs that offer enhanced biological activity and reduced toxicity [30]. In this study, the in vitro antifungal activity of FCZ and its transition metal complexes with glycine was evaluated. The results indicated that both FCZ and its glycine-based metal complexes demonstrated varying degrees of inhibition against the metabolic growth of the tested fungal strains. The size of the inhibition zones reflects the extent of inhibition which is influenced by various factors, including the culture medium, incubation conditions, diffusion rate, and concentration of the antifungal agent. These results suggest that these complexes hold promise as potential candidates for antifungal applications [16]. Fungi such as *Aspergillus niger*, *Penicillium italicum*, and *Candida albicans* have the ability to interact with heavy metal complexes like copper, nickel, and cadmium associated with fluconazole. These interactions depend on several mechanisms, including biosorption, bioaccumulation, and biochemical changes. The fungi have cell walls containing components like chitin, glucosamine, and proteins with functional groups such as carboxyl, amino, and hydroxyl. These functional groups can bind to heavy metal com-

plexes through covalent or ionic bonds. After biosorption, fungi can accumulate these metal complexes within their cells. This accumulation can occur in cellular vacuoles or other organelles like mitochondria. This helps the fungi reduce the toxicity of heavy metals and protect themselves from their harmful effects [31]. Fungi can convert heavy metal complexes into less toxic forms through oxidation and reduction processes. For instance, fungi can convert copper (II) complexes into less toxic forms or insoluble compounds like copper sulfide (CuS) [32].

The data are listed in Table 5 and (Figures 19,20,21), supported by the graphs shown below, where the key color in these graphs represents the different concentrations in milligrams per liter that were used as follows: 2.5, 5, 10, 50, and 100, respectively.

3.4.1. Antifungal Activity of Fluconazole

Aspergillus niger was unaffected by fluconazole at any concentration (Fig. 22). This could be due to resistance mechanisms, such as altered drug binding sites or decreased membrane permeability.

Penicillium italicum (Fig. 23) showed a nearly constant inhibitory zone diameter (6–7 mm) and moderate anti-activity at all concentrations. This implies that flu-

Table 4. XRD spectra data of the principal values of intensity of the FCZ, Gly and their complex with Cu(II)

Compound	2 θ	β (FWHM)	Grain Size D (nm)	Mean D
Fluconazole	9.98	0.156	53.391	36.931
	16.38	0.267	31.397	
	20.04	0.244	34.532	
	25.64	0.259	32.855	
	29.20	0.264	32.478	
Glycine	18.98	0.099	88.591	90.321
	21.82	0.085	103.643	
	25.34	0.082	108.126	
	29.88	0.087	103.384	
	35.90	0.190	47.858	
[Cu(FCZ)(Gly)(H ₂ O) ₂ Cl].2H ₂ O	9.02	0.106	81.861	73.534
	10.54	0.128	67.869	
	14.94	0.115	75.865	
	17.48	0.109	80.516	
	21.36	0.143	61.559	

Table 5. The Antifungal activity of FCZ, Gly and their metal complexes

Compound	mgL ⁻¹	Inhibition zone diameter (mm)		
		<i>Aspergillus Niger</i>	<i>Penicillium italicum</i>	<i>Candida albicans</i>
Fluconazole	2.5	0	7	10
	5	0	7	13
	10	0	7	10
	50	0	6	11
	100	0	6	9
Glycine	2.5	0	7	8
	5	0	7	8
	10	0	7	7.5
	50	0	7	8
	100	0	7	11
[Cu (FCZ)(Gly)(H ₂ O) ₂ Cl].2H ₂ O	2.5	0	0	8
	5	8	0	9
	10	8	0	9
	50	10	0	10
	100	10	0	13
[Ni (FCZ)(Gly)(H ₂ O) ₂ Cl].2H ₂ O	2.5	0	6.5	6
	5	0	10	7
	10	0	7	7
	50	0	7	7.5
	100	9	7	10
[Cd (FCZ)(Gly)(H ₂ O) ₂ Cl].2H ₂ O	2.5	10	15	8
	5	15	16	0
	10	15	16	0
	50	13	16	13
	100	18	25	10
Standard (Nystatin) 100 μ g/ml	100	14	14	13

Reference standard as standard antifungal agent The MIC values are red bold.

conazole has minimal effects that depend on concentration and medium sensitivity.

Candida albicans (Fig. 24): The greatest inhibitory zone (13 mm) was observed at 5 mg/L, suggesting a strong antifungal effect. This is consistent with fluconazole's mechanism of inhibiting cytochrome P450

enzymes that are involved in the synthesis of ergosterol, which renders *C. albicans* more susceptible to it.

3.4.2. Antifungal Activity of Glycine

All studied species showed poor antifungal activity of glycine, suggesting that it is not a naturally strong antifun-

gal agent. However, when used with other substances, it might work as a synergistic agent. At greater concentrations (11 mm at 100 mg/L), there was a minor increase in activity and a slight inhibitory impact against *Candida albicans*. The chelating qualities of glycine, which increase the activity of metal-based compounds, may be the cause of this.

3.4.3. Antifungal Activity of Metal complexes

Cu (FCZ)(Gly)(H₂O)₂Cl].2H₂O

Moderate activity against *Aspergillus niger* was seen with this complex, and inhibition zones expanded to a size of 10 mm at higher concentrations. Copper ions may enhance antifungal activity by generating reactive oxygen species (ROS) that damage fungal membranes. Antifungal activity against *Penicillium italicum* was absent at all concentrations. However, the antifungal activity against *Candida albicans* improved significantly with increasing concentrations, reaching a maximum at 13 mm at 100 mg/L. This illustrates how fluconazole's effects are heightened by copper. By strengthening the inhibitory action on the CYP51 enzyme and elevating oxidative stress, fluconazole linked to copper complexes can be useful in treating infections brought on by this kind of fungus [33].

[Ni (FCZ)(Gly)(H₂O)₂Cl].2H₂O:

In the Ni complex, only a 9 mm inhibitory zone against *Aspergillus niger* was observed at 100 mg/L, indicating modest action. However, a significant activity was seen against *Penicillium italicum* at lower dosages (10 mm at 5 mg/L), and a decline in efficacy at higher concentrations indicated a possible dose-dependent inhibitory mechanism. The inhibitory zones in *Candida albicans* grew somewhat with higher concentrations, reaching 10 mm at 100 mg/L, although overall activity was low to moderate. Nickel complexes associated with fluconazole may be useful in treating *Candida albicans* infections by increasing oxidative stress and enhancing the effects of ordinary fluconazole [31].

[Cd (FCZ)(Gly)(H₂O)₂Cl].2H₂O:

This complex outperformed the conventional Nystatin in terms of activity, with an inhibitory zone diameter of 18 mm at 100 mg/L against *Aspergillus niger* and 25 mm at 100 mg/L. *Penicillium italicum* demonstrated exceptional activity, suggesting that this fungal species is highly sensitive to the cadmium complex. Nevertheless, with *Candida albicans*, the maximum inhibition zone measured 13 mm at 50 mg/L, indicating moderate yet noteworthy action. This illustrates how the reaction varies with concentration. The exceptional effectiveness of this complex implies that cadmium ions significantly increase antifungal activity, either by interfering with fungal proteins or rupturing the integrity of cell membranes. Which agrees with that published that cadmium complexes associated with fluconazole can increase fluconazole's effectiveness in eliminating *Penicillium italicum* by enhancing membrane permeability and oxidative stress [30].

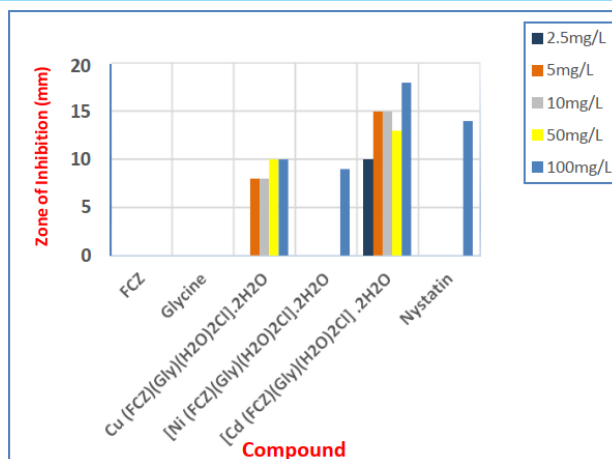


Figure 19. activity of FCZ, Glycine and their metal complexes against *Aspergillus Niger*

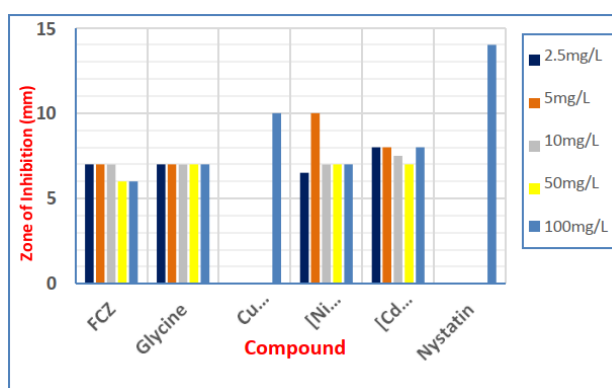


Figure 20. Activity of FCZ, Glycine and their metal complexes against *Penicillium italicum*

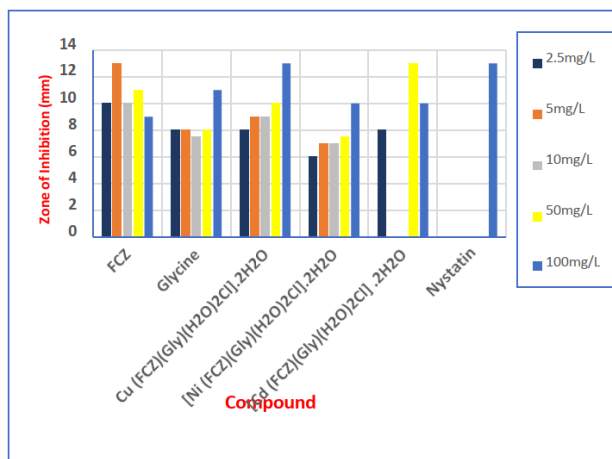


Figure 21. Activity of FCZ, Glycine and their metal complexes against *Candida albicans*

4. CONCLUSION

Fluconazole (FCZ) and its transition metal complexes with glycine were synthesized and thoroughly characterized using various spectroscopic and physicochemical techniques. FCZ has a single coordinating site that is optimally designed to bind transition metals requiring

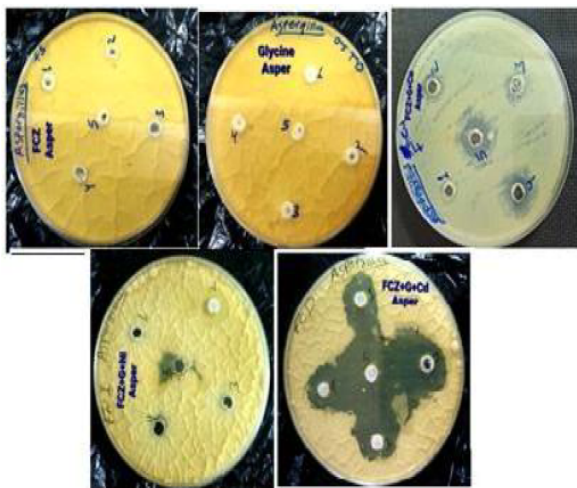


Figure 22. Activity of FCZ drug, Glycine and their metal complexes against *Aspergillus Niger*

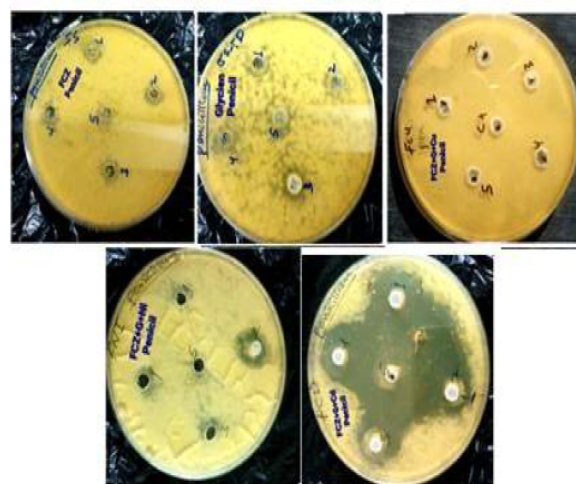


Figure 23. Activity of FCZ drug, Glycine and their metal complexes against *Penicillium italicum*

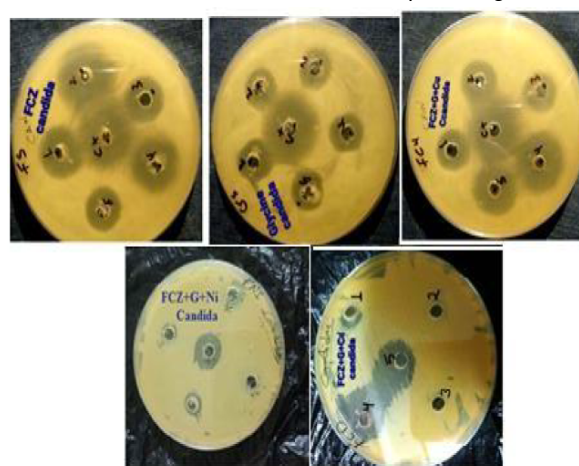


Figure 24. Activity of FCZ drug, Glycine and their metal complexes against *Candida albicans*

octa-coordination. Glycine, an essential amino acid, acts as a bidentate ligand by using its deprotonated carboxylic oxygen and amino group to facilitate coordination with metal ions. These studies provide comprehensive insights into the structural and functional properties of the synthesized complexes. X-ray diffraction (XRD) revealed their crystalline nature, showing smaller mean particle sizes compared to glycine but larger mean particle sizes compared to fluconazole. Notably, further research on their antifungal activity demonstrated that complexing fluconazole and glycine with metals, particularly cadmium $[Cd(FCZ)(Gly)(H_2O)_2Cl] \cdot 2H_2O$, significantly enhanced their antifungal properties. This complex exhibited remarkable antifungal activity, especially against *Aspergillus niger* and *Penicillium italicum*, indicating its potential as a powerful antifungal agent. While glycine and fluconazole alone had limited efficacy, their activity dramatically increased when combined with metals, suggesting that the presence of metals may enhance antifungal effects.

REFERENCES

- [1] A. Garoufis, J. Hatiris, and N. Hadjiliadis. "Ternary complexes of Pt (II) with guanosine and amino acids of the type $trans-[(guo)Pt(amach)Cl]$, where amach is glycine, L-Alanine, L-Valine, and L-Isoleucine". In: *J. Inorg. Biochem.* 41.3 (1991), pp. 195–203. DOI: [10.1016/0162-0134\(91\)80012-7](https://doi.org/10.1016/0162-0134(91)80012-7).
- [2] M. Sabat, K. A. Satyshur, and M. Sundaralingam. "Ternary complexes as models for protein-metal-nucleic acid interactions: structure of palladium (II) complex with glycyl-L-tyrosine and cytidine". In: *J. Am. Chem. Soc.* 105.4 (1983), pp. 976–980. DOI: [10.1021/ja00342a055](https://doi.org/10.1021/ja00342a055).
- [3] A. D. Da Silva et al. "Biological activity and synthetic methodologies for the preparation of fluoroquinolones, a class of potent antibacterial agents". In: *J. Am. Chem. Soc.* 10.1 (2003), pp. 21–39. DOI: [10.2174/0929867033368637](https://doi.org/10.2174/0929867033368637).
- [4] X.-M. Peng, G.-X. Cai, and C.-H. Zhou. "Recent developments in azole compounds as antibacterial and antifungal agents". In: *Curr. Top. Med. Chem.* 13.16 (2013), pp. 1963–2010. DOI: [10.2174/15680266113139990125](https://doi.org/10.2174/15680266113139990125).
- [5] H.-Z. Zhang et al. "New progress in azole compounds as antimicrobial agents". In: *Mini Rev. Med. Chem.* 17.2 (2017), pp. 122–166. DOI: [10.2174/1389557516666160630120725](https://doi.org/10.2174/1389557516666160630120725).



- [6] M. I. Ansari and S. A. Khan. "Synthesis and antimicrobial activity of some novel quinoline-pyrazoline-based coumarinyl thiazole derivatives". In: *Med. Chem. Res.* 26 (2017), pp. 1481–1496. DOI: [10.1007/s00044-017-1855-4](https://doi.org/10.1007/s00044-017-1855-4).
- [7] M. Ali et al. "Fluconazole and its interaction with metal (II) complexes: SEM, spectroscopic and antifungal studies". In: *Pak. J. Pharm. Sci.* 30.1 (2017).
- [8] N. Lj. Stevanović et al. "Copper (II) and zinc (II) complexes with the clinically used fluconazole: comparison of antifungal activity and therapeutic potential". In: *Pharmaceuticals* 14.1 (2020), p. 24. DOI: [10.3390/ph14010024](https://doi.org/10.3390/ph14010024).
- [9] P. Keerthika, S. Balasubramanian, and R. Govindharaju. "Diamagnetic Zn (II) and Hg (II) complexes with fluconazole: Synthesis, spectral characterization and biological investigation". In: *Biosci. Biotechnol. Res. Asia* 20.2 (2023), pp. 681–689. DOI: [10.13005/bbra/3122](https://doi.org/10.13005/bbra/3122).
- [10] K. Stryjska et al. "Synthesis, spectroscopy, single-crystal structure analysis and antibacterial activity of two novel complexes of silver (I) with miconazole drug". In: *Int. J. Mol. Sci.* 22.4 (2021), p. 1510. DOI: [10.3390/ijms22041510](https://doi.org/10.3390/ijms22041510).
- [11] Z. H. Chohan, C. T. Supuran, and A. Scozzafava. "Metal binding and antibacterial activity of ciprofloxacin complexes". In: *J. Enzym. Inhib. Med. Chem.* 20.3 (2005), pp. 303–307. DOI: [10.1080/14756360310001624948](https://doi.org/10.1080/14756360310001624948).
- [12] Z. H. Chohan et al. "Antibacterial role of SO₂, NO, CO₂ and CHCO anions on Cu (II) and Zn (II) complexes of a thiadiazole-derived pyrrolyl Schiff base". In: *Met. Drugs* 8.5 (2002), pp. 263–267. DOI: [10.1155/MBD.2002.263](https://doi.org/10.1155/MBD.2002.263).
- [13] F. Klavs. *Analytical Profiles of Drug and Excipients*. Vol. 27. New Jersey, USA: Academic Press, 1987, pp. 67–112.
- [14] A. Singh, P. K. Sharma, and D. K. Majumdar. "Development and validation of different UV-spectrophotometric methods for the estimation of fluconazole in bulk and in solid dosage form". In: *IJCT* 18.5 (Sept. 2011). URL: <http://nopr.niscares.in/handle/123456789/13030>.
- [15] Pfizer Australia Pty Ltd. *Diffucan (Australian Approved Product Information)*. West Ryde, NSW, Australia: Pfizer Australia, 2004.
- [16] Y. M. Jamil et al. "Spectroscopic and biological studies of mixed ligand complexes of transition metal (II) ions with chloroquine and ketoprofen". In: *JAST* 2.1 (Feb. 2024), pp. 53–64. DOI: [10.59628/jast.v2i1.801](https://doi.org/10.59628/jast.v2i1.801).
- [17] F. M. Al-Azab et al. "Titanium Complex with New Schiff Base 4-(N, N-dimethylaminobenzylidene)-1-phenylsemicarbazide: Synthesis, Thermal, XRD, and Antibacterial properties". In: *JAST* 2.4 (Sept. 2024), pp. 391–402. DOI: [10.59628/jast.v2i4.1145](https://doi.org/10.59628/jast.v2i4.1145).
- [20] T. O. Aiyelabola et al. "Synthesis, characterization and antimicrobial activities of some metal (II) amino acids' complexes". In: *Adv. Biol. Chem.* 2.3 (2012), pp. 268–273. DOI: [10.4236/abc.2012.23034](https://doi.org/10.4236/abc.2012.23034).
- [21] A. A. Latha et al. "Synthesis and characterization of -glycine—a nonlinear optical single crystal for optoelectronic and photonic applications". In: *Mater. Sci.* 35.1 (2017), pp. 140–150. DOI: [10.1515/msp-2017-0031](https://doi.org/10.1515/msp-2017-0031).
- [18] G. G. Mohamed et al. "Synthesis and characterization of mixed ligand complexes of lomefloxacin drug and glycine with transition metals. Antibacterial, antifungal and cytotoxicity studies". In: *J. Mol. Struct.* 999.1–3 (2011), pp. 29–38. DOI: [10.1016/j.molstruc.2011.05.018](https://doi.org/10.1016/j.molstruc.2011.05.018).
- [19] J. Han and Y. S. Chi. "Vibrational and electronic spectroscopic characterizations of amino acid-metal complexes". In: *J. Korean Soc. for Appl. Biol. Chem.* 53 (2010), pp. 821–825. DOI: [10.3839/jksabc.2010.124](https://doi.org/10.3839/jksabc.2010.124).
- [22] N. S. Al-Radadi et al. "Synthesis, spectroscopic characterization, molecular docking, and evaluation of antibacterial potential of transition metal complexes obtained using triazole chelating ligand". In: *J. Chem.* 2020 (2020). DOI: [10.1155/2020/1548641](https://doi.org/10.1155/2020/1548641).
- [23] W. A. Mahmoud, Z. M. Hassan, and R. W. Ali. "Synthesis and spectral analysis of some metal complexes with mixed Schiff base ligands 1-[2-(2-hydroxybenzylideneamino) ethyl] pyrrolidine-2,5-dione (HL) and (2-hydroxybenzalidine) glycine (HL)". In: *Journal of Physics: Conference Series*. Vol. 1660. 1. 2020, p. 012027. DOI: [10.1088/1742-596/1660/1/012027](https://doi.org/10.1088/1742-596/1660/1/012027).
- [24] R. Gopalan. *Inorganic Chemistry for Undergraduates*. Hyderabad, India: Universities Press, 2009.
- [25] L. A. Karem. "Synthesis, characterization and biological evaluation of new Schiff bases mixed ligand metal complexes of some drug substances". M.S. thesis. Baghdad, Iraq: College of Education for Pure Sciences, Univ. Baghdad, 2016.
- [26] B. D. Cullity. *Elements of X-Ray Diffraction*. 2nd. Reading, MA, USA: Addison-Wesley, 1978, pp. 127–131.
- [27] Y. M. Jamil et al. "Preparation, physicochemical characterization, molecular docking and biological activity of a novel Schiff-base and organophosphorus Schiff base with some transition metal(II) ions". In: *Main Group Chem.* 22.3 (2023), pp. 337–362. DOI: [10.3233/MGC-220101](https://doi.org/10.3233/MGC-220101).
- [28] S. R. Desai and S. R. Dharwadkar. "Study of process induced polymorphic transformations in fluconazole drug". In: *Microsc. Res. Tech.* 72.9 (2009), pp. 702–710. DOI: [10.1002/jemt.20715](https://doi.org/10.1002/jemt.20715).
- [29] S. A. Chudar and S. Ganesan. "Crystal growth, structural, optical, thermal and NLO studies of -glycine single crystals". In: *Optik* 124.23 (2013), pp. 6456–6460. DOI: [10.1016/j.ijleo.2013.05.030](https://doi.org/10.1016/j.ijleo.2013.05.030).
- [30] A. S. I. Ali et al. "Metal (II) Complexes of Fluconazole: Thermal, XRD and Cytotoxicity Studies". In: *Iran. J. Pharm. Res.* 19.3 (2020), e124396. DOI: [10.22037/ijpr.2020.1101142](https://doi.org/10.22037/ijpr.2020.1101142).
- [31] M. Q. Qader and Y. A. Shekha. "Bioremediation of heavy metals by using *Aspergillus niger* and *Candida albicans*". In: *Zanco J. Pure Appl. Sci.* 35.3 (2023), pp. 180–186. DOI: [10.21271/ZJPAS.35.3.18](https://doi.org/10.21271/ZJPAS.35.3.18).
- [32] G. M. Gadd. "Geomycology: Biogeochemical transformations of rocks, minerals, metals and radionuclides by fungi, bio weathering and bioremediation". In: *Mycol. Res.* 111.1 (Jan. 2007), pp. 3–49. DOI: [10.1016/j.mycres.2006.12.001](https://doi.org/10.1016/j.mycres.2006.12.001).
- [33] S. Sharma and A. Gupta. "Metal-based antifungal agents: A review". In: *Eur. J. Med. Chem.* 156 (2018), pp. 1–15. DOI: [10.1016/j.ejmech.2018.06.055](https://doi.org/10.1016/j.ejmech.2018.06.055).